ELSEVIER

Journal of Alloys and Compounds 404–406 (2005) 16–23

Journal of ALLOYS AND COMPOUNDS

www.elsevier.com/locate/jallcom

Some thermodynamic aspects of metal hydrogen systems

T.B. Flanagan[a,*], W.A. Oates[b]

[a] *Department of Chemistry, University of Vermont, Burlington, VT 05405, USA*
[b] *Department of Materials, University of Salford, Salford, UK*

Received 7 September 2004; accepted 8 November 2004
Available online 12 July 2005

Abstract

The various degrees of equilibrium which are possible in the two-phase co-existence region of metal hydride systems will be reviewed. Some of these lead to invariant p_{H_2} and others to sloping plateaux. The effect of hysteresis on the thermodynamic properties of metal hydrides is discussed. Recent advances in theoretical first principle calculations of the energy of hydride formation are reviewed.

Keywords: Thermodynamics; Plateau sloping; Hysteresis; Calorimetry

1. Introduction

For most researchers the thermodynamic aspects of metal hydride systems are limited to plots of log of the plateau pressures against $1/T$, van't Hoff plots, whereby ΔH_{plat} and ΔS_{plat} are determined. There are, however, many other aspects of the thermodynamics of these systems and some of these will be considered in this paper with a main focus on the plateau region. Firstly, the different degrees of equilibrium possible in the two-phase co-existence region of metal hydride systems will be discussed because these determine the plateau behavior. The following pertains to random, substitutional alloys or to non-stoichiometric intermetallic compounds. The three possible situations for a two solid phase region in A–B–H systems are: complete equilibrium, CE, local equilibrium, LE, and "frozen" metal/mobile H atom, PE, para-equilibrium. In all of these the condition $\mu_H(\alpha) = \mu_H(\beta)$ is satisfied because of the mobility of the H atoms. The frozen metal situation (PE) is the one that is almost universally found in alloy hydrides since they are studied and employed at moderate temperatures. A preliminary discussion of these equilibria for metal–H systems appeared in ref. [1].

2. Classification of two-phase equilibrium

2.1. Complete equilibrium (CE)

In CE, the chemical potentials of each species in a phase must be equal to those in co-existing phases. For a binary M–H system the equality of the chemical potentials leads to a plateau pressure and the absence of sloping or hysteresis as shown in Fig. 1. It should be noted that μ_M is a function of $r = n_H/n_M$. The co-existing phase boundaries are shown as a and b for a binary system at CE (Fig. 1).

CE can occur in a ternary system A–B–H such as a substitutional alloy Pd–Pt–H, where it is assumed that it does not separate into PdH and Pt phases at equilibrium but, instead, into Pd-rich and -poor phases, which is consistent with the experimental finding that such a separation does occur at moderately high temperatures and hydrogen pressures [2]. In the case of a non-stoichiometric intermetallic compound, e.g., AB_{2+x}, it is assumed that there is a limited CE where the intermetallic separates into two AB_{2+x}–H phases with different x values rather than completely into AH and B.

There are two compositional variables for a ternary system, r, and c_B where $c_B = n_B/(n_A + n_B)$, where the n_I are mols. A diagram, such as Fig. 1, cannot be drawn for a ternary system under CE conditions. A representation, such as shown in Fig. 2, can be employed, however, where the abscissa is

* Corresponding author. Tel.: +1 802 656 0199; fax: +1 802 656 8705.
E-mail address: flanagan@emba.uvm.edu (T.B. Flanagan).

0925-8388/$ – see front matter © 2005 Elsevier B.V. All rights reserved.
doi:10.1016/j.jallcom.2004.11.108

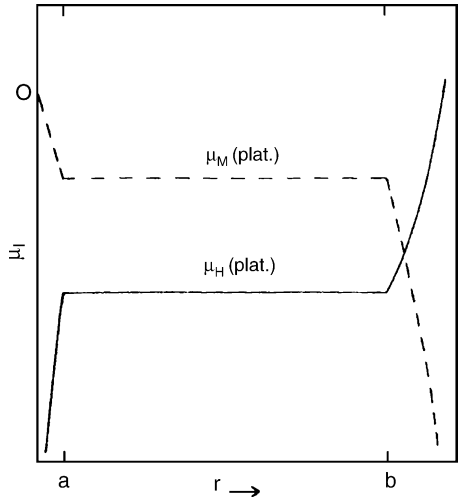

Fig. 1. Schematic plot of μ_I against r = H/M under isothermal conditions where I = H and M = metal.

c_B and the ordinate is r and constant μ_I values are shown by the different tie-lines in the two-phase field connecting the α, dilute, and β, hydride, phases which are shown by the two solid lines enclosing the two-phase field. The tie-lines continue into the single-phase regions where the μ_I are also constant. The vertical dashed line is the overall alloy composition, c_o. The fraction of β, f_β, increases as r increases across the two-phase field. The sloping of the tie-lines in the two-phase field will decrease as c_B for a substitutional alloy approaches the pure metal A or the stoichiometric composition for an intermetallic compound.

Upon increasing the H content in the α phase, the hydride phase first appears at point 1 where the α phase of that composition will co-exist, according to the tie-line (1–2), with a different bulk metal atom composition in the β shown by 2. The overall metal atom composition must be maintained at

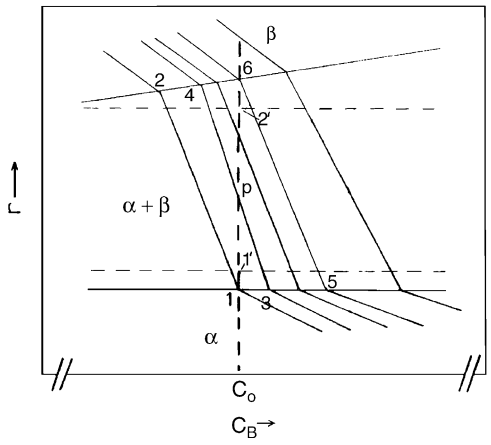

Fig. 2. Schematic representation of the two-phase co-existence region for a ternary system. The nearly horizontal solid lines are phase boundaries for CE and the other solid lines are iso-chemical potential tie-lines in the single-phase and two-phase regions. The vertical dashed line at c_o is the overall alloy content and the horizontal dashed lines are the phase boundaries for PE.

c_o so that f_β is ≈0 at point 1. When the H content is increased within the two-phase field to point p where $f_\beta = \frac{1}{2}$, the tie-line (3–4) gives the metal compositions 3 and 4 for the α and β phases, respectively. The overall composition of the alloy is maintained as reflected by equal excursions on the two sides of c_o. Finally, when conversion to the β phase is nearly complete, the tie-line (5–6) shows that the α composition corresponds to 5 and the β to 6. For CE, the chemical potentials of *all* components are equal along any of the tie-lines within the two-phase field.

The tie-lines intersected as f_β increases correspond to increasing H contents of the two co-existing phases because they intersect the β phase boundary at progressively larger H contents.

The changes in the α phase H contents will be smaller and are therefore not indicated by a sloping phase boundary. The μ_H must also increase with f_β because of the thermodynamic stability requirement, $(\partial\mu_H/\partial n_H)_T > 0$ [3]. Another proof of this is that in the α phase as n_H increases at constant c_B tie-lines are crossed of increasing μ_H and the extensions of these into the two-phase field shows that when f_β increases, μ_H must also increase. Since μ_H increases with f_β in the two-phase field according to both of these arguments, there will be *no* plateau pressure for these ternary systems under CE, i.e., "sloping plateaux" are expected.

2.2. "Frozen" metal /mobile H atoms (PE)

In this case, the immobility of the metal atoms in the bulk and interface precludes the establishment of CE and this has been designated as para equilibrium (PE). Ternary hydrides which fall into this category are also referred to as psuedo-binary hydrides [4].

For *binary* M–H systems Fig. 1 describes both CE and PE conditions because it is not necessary for the metal atoms to be mobile in order for $\mu_M(\alpha) = \mu_M(\beta)$ since the μ_M depend on their H contents. On the other hand, for *ternary* systems different results obtain under PE than CE. In Fig. 2, the horizontal dashed lines represent the PE phase boundaries which must lie within the CE boundaries [5]. When H_2 is added to the alloy, it dissolves in the dilute phase until, at the phase boundary, 1′, hydride phase at 2′ appears and the metal compositions of both of these phases are equal to c_o corresponding to the dashed vertical line where the PE system remains as f_β increases and along this vertical dashed line the chemical potentials for H and for M in both phases are equal and constant until the α phase is fully hydrided at 2′. Fig. 1 is applicable to this "frozen" metal/mobile H atom situation which obtains at moderate temperatures for alloy and intermetallic–H systems. PE leads to the desirable invariant μ_{H_2}, a plateau p_{H_2}, across the two-phase field. Although the metal atoms are "frozen", the $\mu_M(\alpha) = \mu_M(\beta)$ condition can be satisfied, as for the binary case, because μ_M are a function of the H content of each phase. As for the binary systems, the metal atom immobility may cause stresses leading to plateau sloping and hysteresis.

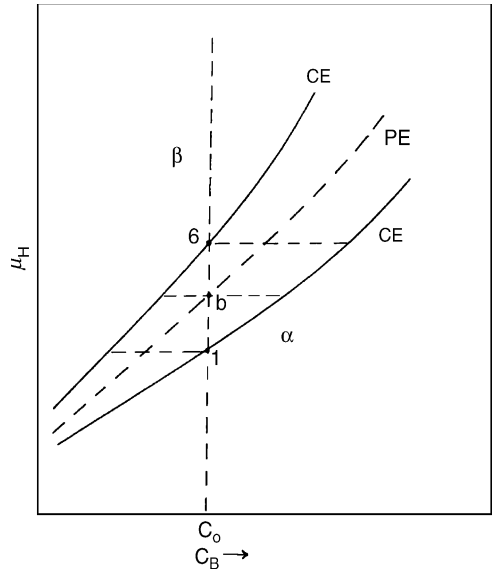

Fig. 3. Schematic plots of μ_H against c_B for CE and PE. Point b is the constant μ_H plateau for PE but for CE, μ_H increases from 1 to 6 during hydriding from f_β=0 to 1.0.

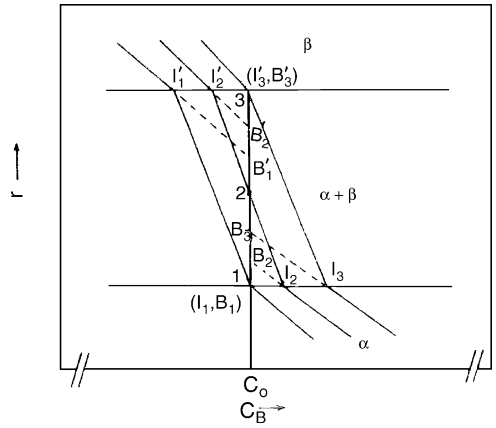

Fig. 4. Schematic representation of the two-phase co-existence region for LE. I and I' represent the interface compositions in the α and β phases, respectively. B and B′ are the bulk compositions in the α and β phases, respectively. The horizontal solid lines are phase boundaries and the vertical solid line is the overall alloy composition c_o and the bulk compositions must remain on this for PE. The other solid lines are iso-chemical potential tie-lines as in Fig. 2 and are applicable to the interface. The dashed lines are tie-line extensions from the single-phase regions to c_o.

Fig. 3 is a schematic plot of μ_H against c_B for CE and PE. For PE, μ_H remains at b while f_β changes from 0 to 1. By contrast, for CE μ_H changes from 1 ($f_\beta = 0$) to 6 ($f_\beta = 1$) and the metal atom compositions of the co-existing phases also change according to the intersections of the dashed horizontal lines with the CE phase boundaries shown by the solid lines.

2.3. Partial or local equilibrium (LE)

In local equilibrium (LE) the metal atoms are in equilibrium at the interface but not in the bulk where they are "frozen" as for PE. The mobile H atoms, however, are at equilibrium throughout the system. This is illustrated schematically in Fig. 4 where again the overall H content, r, is plotted against c_B. I_I and B_I represent compositions at the interface and the bulk, respectively. The phase boundaries are shown by the horizontal solid lines. The values of c_B in the co-existing bulk phases are fixed at c_o because of the immobility of the metal atoms in the bulk phases. The non-vertical lines in the two-phase field are iso-chemical potential tie-lines for the co-existence of the two phases. Their extensions into the single-phase regions are shown. The dashed lines within the two-phase field are extensions of the single-phase iso-chemical potential tie-lines.

Upon entering the two-phase field at 1 (Fig. 4) the bulk and interface compositions of the α phase are the same (B_1, I_1) but this is not the same for the β phase where the bulk (B'_1) and interface (I'_1) compositions differ. With increase of f_β within the two-phase field, the bulk metal compositions will always remain at c_o but the interface will vary with f_β. At 2, where $f_\beta = \frac{1}{2}$ the α phase interface and bulk compositions are I_2 and B_2, respectively, while the co-existing β phase compositions are I_2 and B_2. These β phase compositions are obtained by drawing an iso-chemical potential tie-line through 2 as shown (Fig. 4) which intersects the phase boundaries to give the interface compositions similarly to the case of CE (Fig. 2). At any point within the two-solid phase field $\mu_H(\alpha) = \mu_H(\beta)$, for instance, at 2 (Fig. 4) all of the co-existing compositions lie on the tie-line (I_2–I'_2) or else on the dashed line extensions into the two-phase region intersecting c_o at B_2 and B'_2. When the sample is almost fully hydrided at 3, the composition of the interface is I_3 and the bulk phase B'_3 are the same.

It can be seen (Fig. 4) that the H compositions of the bulk phases increase with f_β, for example, the H concentration for the α phase at 1 is B_1 and the β phase is B'_1 and at 2, the corresponding concentrations are B_2 and B'_2, i.e., the bulk concentrations of H increase with f_β and therefore μ_H must increase in accord with thermodynamic principles [3]. Since μ_H increases with increasing H concentration in the two-phase field, the plateau slopes. LE at the interface was first discussed by Oates and Flanagan [1] as a possible source of plateau sloping in metal alloy–H and intermetallic–H systems.

The model of LE must be modified under some conditions where c_B becomes equal to c_o on the β side of the interface *before* $f_\beta = 1$ and therefore the plateau would not slope in this region. The following conditions contribute to $c_B = c_o$ at the β side of the interface for $f_\beta < 1$ [6]: large particle size, a small difference ($c_B - c_o$) at I'_1 (Fig. 4) and a small thickness of the pile-up on the α-side of the interface. In the above discussion it was assumed that these conditions are *not* fulfilled and $c_B = c_o$ only at $f_\beta = 1$ which seems most likely for nano-sized samples.

Even under conditions where c_o is reached at small values of f_β, LE can play a role in metal hydride systems. For instance, Park and Flanagan [6] utilized the concept of LE to ex-

plain the "aliquot effect" in $LaNi_7$ [7] whereby fast interface velocities lead to lower hydride formation plateau pressures than slow velocities. In this case, the plateaux are relatively flat and therefore it was assumed that the β phase composition at the interface became equal to c_o at a relatively small value of f_β.

3. Plateau thermodynamic parameters vis-à-vis hysteresis

The following applies to most practical situations for metal hydrides where a plateau is present, i.e., PE obtains because under CE conditions there would be no plateaux for ternary systems. Since PE is the dominant situation and it gives rise to plateaux, some discussion of plateau thermodynamics is pertinent.

3.1. Plateau enthalpies

3.1.1. Calorimetrically determined enthalpies

Calorimetrically measured enthalpies do not depend on the attainment of equilibrium p_{H_2} but only on the heats evolved/absorbed which are essentially independent of p_{H_2} provided that the H_2 behaves ideally and hydrostatic effects are nil. It should be recalled that most calorimetric determinations of enthalpies of chemical reactions are carried out under irreversible conditions. If hydride formation and decomposition are the exact reverses of each other, their calorimetric enthalpies must be equal in magnitude. This will not be strictly true because the phase boundaries are not the same for hydride formation and decomposition, but this is generally a second order effect and the calorimetric enthalpy magnitudes are very closely equal at moderate p_{H_2}. High precision calorimetry shows that for ZrNi–H, which has a large hysteresis, the hydride formation and decomposition values of $|\Delta H_{plat}|$ are equal [8] and the same is true for Pd–H(D) [9] and $LaNi_5$–H [10].

It is of interest to understand why calorimetrically determined enthalpies are unaffected by hysteresis. Fig. 5 shows an isothermal schematic system exhibiting hysteresis where the phase boundaries a and b expressed as atom ratios, r, are assumed to be unaffected by hysteresis and, for convenience, a and b are taken as 0 and 1, respectively. The equilibrium pathway is shown for convenience in the center of the normal hysteresis gap; it cannot be located above p_f or below p_d because then the assumed irreversible steps, $(1' \rightarrow 2')$ and $(4' \rightarrow 5')$, would not generate entropy.

Pathways with initial and final states labelled with primes are irreversible and those with unprimed or a mixture of prime and unprimed states are reversible. The hypothetical reversible step $(6 \leftrightarrow 3)$, which does not have to exist for a real system, corresponds to reversible hydride formation and decomposition according to reaction (1):

$$\tfrac{1}{2}H_2(p_{H_2,eq}) + M = MH. \quad (1)$$

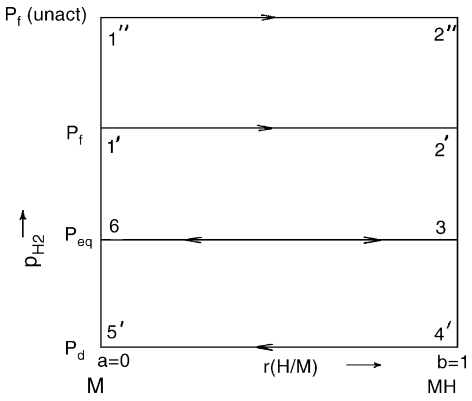

Fig. 5. Schematic diagram of reversible and irreversible paths for hydride formation and decomposition for reaction (1). The upper, irreversible path $1'' \rightarrow 2''$ is for unactivated material and the next lower one, $1' \rightarrow 2'$, is for hydriding the activated form.

Since enthalpy is path-independent it is clear that if the H_2 is ideal and the process is isothermal,

$\Delta H(1' \rightarrow 6) = \Delta H(3 \rightarrow 2') = 0$ and therefore $\Delta H(1' \rightarrow 2') = \Delta H(6 \rightarrow 3) = \Delta H^{f}_{plat,eq}$. The same argument can be made for hydride decomposition giving $\Delta H(4' \rightarrow 5') = \Delta H(3 \rightarrow 6) = \Delta H^{d}_{plat,eq}$. Because it has been assumed that equilibrium hydride formation and decomposition are the exact reverses of each other, the calorimetrically measured enthalpies for hydride formation and decomposition must have the same magnitude. i.e.,

$$|\Delta H(6 \rightarrow 3)| = |\Delta H(3 \rightarrow 6)| = |\Delta H_{plat,eq}|.$$

It is also instructive to consider the heats for hydride formation/decomposition using the reversible steps because they can be evaluated. The sum of the heats (per mol H) for hydride formation $(1' \rightarrow 2')$ from the reversible pathways (Fig. 5) is given by Eq. (2):

$$(1' \rightarrow 2')(\text{rev. paths.}) = (1' \rightarrow 6) + (6 \rightarrow 3) + (3 \rightarrow 2') = RT \ln\left(\frac{p_f}{p_{eq}}\right)^{1/2} + q_{eq} + 0 \quad (2)$$

and $q_{eq} = -|\Delta H_{plat,eq}|$. The irreversible step $(1' \rightarrow 2')$ is, however, accompanied by a heat evolution from the conversion of the driving force into heat, $= -RT \ln(p_f/p_{eq})^{1/2}$, which enters the surroundings cancelling the heat for the reversible step $(1' \rightarrow 6)$. The total heat change for the irreversible hydride formation $(1' \rightarrow 2')$ is therefore $q_{eq}(6 \rightarrow 3)$ which is equal to $-|\Delta H_{plat,eq}|$; this shows that the driving force is evolved as heat from the overcoming of obstacles causing the hysteresis. Similar arguments can be made for the decomposition step where there is also a driving force converted to a heat.

The same argument can be applied to the initial hydriding cycle of, e.g., $LaNi_5$, where p_f, initial is much greater than for subsequent hydriding as reported first by Flanagan and Biehl [11]. It was found by Luo et al. [12] that

the calorimetric enthalpy for the initial hydriding (activation) was the same as for subsequent ones despite the large difference in their plateau pressures because the arguments are not affected by the specific values of p_f (Fig. 5). The reversible heat for the step ($1'' \rightarrow 2''$) (Fig. 5) is RT $\ln(p_f, \text{initial}/p_{eq})^{1/2} - |\Delta H_{plat,eq}|$ and the heat dissipated by the driving force is $-RT \ln(p_{f,initial}/p_{eq})^{1/2}$ and therefore the heat for the irreversible step ($1'' \rightarrow 2''$) taking place at the initial high p_f is again $q_{eq}(6 \rightarrow 3) = -|\Delta H_{plat,eq}|$ despite the fact that the initial cycle causes the alloy to disintegrate into small particles. Any heat evolution accompanying the disintegration returns to the surroundings and any energy which is not evolved due to creation of new surface is relatively unimportant for the AB_5 intermetallics.

3.2. Plateau enthalpies from van't Hoff plots

The majority of thermodynamic data are derived from van't Hoff plots of the plateau p_{H_2} which are directly affected by hysteresis. In some M–H systems hysteresis is very large, e.g., for $CeNi_5$–H, $RT \ln(p_f/p_d)^{1/2} = 1.9$ kJ/mol H and the plateau enthalpies obtained from the van't Hoff plots are $\Delta H^f_{plat} = -8.35$ kJ/mol H and $\Delta H^d_{plat} = 11.1$ kJ/mol H [13], i.e., their magnitudes differ by 25%. In other words, there can be large differences between the van't Hoff determined values for hydride formation and decomposition.

Since the plateau p_{H_2} are directly influenced by hysteresis, it seems obvious that the van't Hoff plots should be affected. It is instructive to examine this quantitatively starting from the identity

$$RT \ln p_f^{1/2} = RT \ln \left(\frac{p_f}{p_{eq}}\right)^{1/2} + RT \ln p_{eq}^{1/2} \quad (3)$$

where the first term on the right-hand-side represents hysteresis for hydride formation ($1' \rightarrow 2'$) and will be indicated as (hyst $\times$ f_f) where f_f is the fraction of the total hysteresis due to hydride formation and, it is important to note, hysteresis does not change much with temperature unless the temperature range is significant enough to change the phase boundaries, e.g., near the critical temperature. For example, from the data of Lasser and Klatt [14] for Pd–H, hysteresis, $RT \ln(p_f/p_d)^{1/2} = 740$ J/mol H at 343 K and 766 J/mol H at 423 K. Since this is nearly temperature independent, Eq. (3) can be re-written after division by T as:

$$R \ln p_f^{1/2} = \frac{(\text{hyst} \times f_f)}{T} + R \ln p_{eq}^{1/2} \quad (4)$$

and differentiation with respect to $1/T$, gives:

$$R\left(\frac{\partial \ln p_f^{1/2}}{\partial(1/T)}\right) = (\text{hyst} \times f_f) + R\left(\frac{\partial \ln p_{eq}^{1/2}}{\partial(1/T)}\right) \quad (5)$$

or

$$\Delta H^f_{plat} = (\text{hyst} \times f_f) + \Delta H^f_{plat,eq} \quad (6)$$

If a similar procedure is carried out for $RT \ln p_d^{1/2}$, Eq. (7) is obtained:

$$\Delta H^d_{plat} = (\text{hyst} \times f_d) + \Delta H^d_{plat,eq} \quad (7)$$

where the signs of ΔH are negative for hydride formation and positive for decomposition. If Eqs. (6) and (7) are added:

$$\Delta H^f_{plat} + \Delta H^d_{plat} = \text{hyst} = RT \ln \left(\frac{p_f}{p_d}\right)^{1/2} \quad (8)$$

because $f_f + f_d = 1$. It should be noted that $|\Delta H^f_{plat}| < |\Delta H^d_{plat}|$ follows from Eqs. (6) and (7) since the hyst.term is always positive and this inequality is found experimentally. These conclusions hold for both alloys and intermetallic hydride systems.

3.3. Plateau entropies

The entropy change for reaction (1) where $p_{H_2} = p_{H_2,eq}$ is given by

$$\Delta S_{plat,eq} = \frac{\Delta H_{plat,eq}}{T} \quad (9)$$

where $\Delta H_{plat,eq}$ is the equilibrium value, i.e., one from calorimetry or else, if this is not available, an average magnitude from the two van't Hoff plots would be a good approximation to $\Delta H_{plat,eq}$. As seen from Eq. (9) this equilibrium entropy clearly depends on temperature.

The usual entropies determined from van't Hoff plots, however, are not for $p_{H_2} = p_{H_2,eq}$ (reaction (1)) but for $p_{H_2} = 1$ bar. The H_2 is in its standard state for this entropy change, $\Delta S_{plat,1\,bar}$, but since non-stoichiometric solid phases are not considered as standard states, a designation reserved for stoichiometric hydrides, $\Delta S_{plat,1\,bar}$ would not be a standard value. In M–H solutions, the infinitely dilute solution is taken as the standard state.

For reaction (1) with $p_{H_2} = 1$ bar, the $\Delta S_{plat,1\,bar}$ can be derived from calorimetry using:

$$\Delta S_{plat,1\,bar} = \frac{\Delta H_{plat,cal}}{T} - R \ln(p_{plat,eq})^{1/2} \quad (10)$$

where $p_{plat,eq}$ is approximated by $(p_f p_d)^{1/2}$ and $\Delta H_{plat,cal} = \Delta H_{plat,eq}$. The last term in Eq. (10) is the entropy for changing p_{H_2} from $p_{plat,eq}$ to 1 bar. Since the $\Delta H_{plat,cal}/T$ term is unaffected by hysteresis, it is desirable to also remove the effect of hysteresis from the p_{H_2} term and the use of the geometric mean appears to accomplishes this. Fig. 6 shows desorption data for Pd–H where $(\Delta H_{plat,eq}/T)$, R ln $p_{eq}^{1/2}$ and their sum are plotted against T. It can be seen that the addition of the first two quantities gives a $\Delta S_{plat,1\,bar}$ nearly independent of temperature. Similar plots may be made for other M–H systems.

Curiously, $\Delta S_{plat,1\,bar}$ values derived from van't Hoff plots do not appear to be affected by hysteresis while the ΔH_{plat} values *are* affected [15]. If Eq. (3) is differentiated with respect to T, $-\Delta S^f_{plat,1\,bar}$ is obtained because $RT \ln p_f^{1/2}$ is the

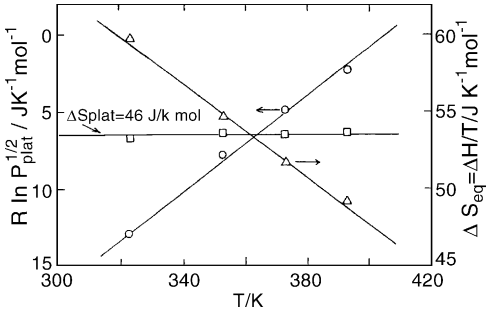

Fig. 6. Illustration of entropy changes for reaction (1) for $p_{H_2} = p_{H_2}$ (eq) or $= p_{H_2}$ (1 bar) using desorption data for Pd–H, ΔS_{plat} ($p_{H_2} = 1$ bar); Δ, ΔS_{plat} ($p_{H_2,eq}$), (◯) $R \ln p^{1/2}$.

Gibbs free energy change for reaction (1) or a more general version of it where $a \neq 0$ and $b \neq 1$:

$$-\Delta S^{f}_{plat,1\,bar} = R\left(\frac{d(T \ln p_f^{1/2})}{dT}\right)$$

$$= R \ln(p_{plat,eq})^{1/2} + RT\left(\frac{d \ln p_{eq}^{1/2}}{dT}\right) \quad (11)$$

where $\Delta S_{plat,1\,bar}$ refers to an entropy change at 1 bar unaffected by hysteresis rather than to the value for reaction (1) at $p_{plat,eq}$ and it has been assumed, as above, that $d(hyst \times f_f)/dT) = 0$. It can also be shown for hydride decomposition that the $\Delta S^{d}_{plat,1\,bar}$ obtained from the van't Hoff plot is also independent of hysteresis. Thus, the van't Hoff-determined $|\Delta S_{plat}|$ values for hydride formation and decomposition should be equal to each other but the $|\Delta H_{plat}|$ should not be.

In contrast to most metal–H systems, the data for Pd–H are sufficiently accurate to test these thermodynamic arguments. For example, $|\Delta H^{f}_{cal,plat}| = |\Delta H^{d}_{cal,plat}| = 19.1 \pm 0.2$ kJ/mol H from reaction calorimetric measurements at 298 K [10]. The most accurate thermodynamic data from *p–c–T* measurements for Pd–H were obtained by Lasser and Klatt [14] where complete isotherms were measured at 15 different temperatures from 323 to 393 K giving $|\Delta H_{plat}| =$ 19.5 and 18.7 kJ/mol H for hydride decomposition and formation, respectively. The average of their enthalpy magnitudes values is 19.1 kJ/mol H agreeing almost exactly with that from reaction calorimetry [10]. The difference between these two magnitudes from the van't Hoff plots is 0.8 kJ/mol H which is in good agreement with the prediction from Eq. (8) that this should be equal to hysteresis for Pd–H and its value at the average temperature of their measurements, 383 K, is RT ln $(p_f/p_d)^{1/2} = 0.79$ kJ/mol H. The magnitudes of the entropy changes derived from the van't Hoff plots by Lasser and Klatt are 46.3 and 46.2 J/K mol H for hydride formation and decomposition, respectively [14]. The value from calorimetry is 46.6 J/K mol H [10] using Eq. (10) and $p_{plat,eq} = (p_f p_d)^{1/2}$. Thus, data for this classical metal–H system conform remarkably well with the thermodynamic predictions.

3.4. Some recent theoretical developments

Electronic structure calculations on metal–hydrogen systems prior to about 1980 (for a review see [16]) gave little information about the lattice stability of hydrides or the preferred site for occupation by the hydrogen atoms. Knowledge of the latter is important in any thermodynamic modeling of a phase and, in earlier times, was often based on simple geometric concepts [17].

In 1986, Nordlander et al. [18] made a more sophisticated analysis by carrying out jellium-type calculations. It was suggested that H atoms attempt to occupy positions where the electron density is such as to make the embedding energy most exothermic. In the majority of metals this coincides with H occupying the tetrahedral (T) sites (bcc metals) and octahedral (O) sites (hcp and fcc). In certain metals, however, the generalization appeared to break down and it was of little value for site occupancy in intermetallic compounds.

The situation has changed dramatically in the past few years with the use of calculations based on ab initio density functional theory [19,20]. These calculations are capable of providing a much more complete picture for the thermodynamicist, i.e., lattice parameters, site occupation, stability elastic properties, zero point energies and phonon spectra can all be calculated (see [21–27]). Although the Vienna Ab Initio Simulation Package (VASP) [28] has mostly been used in these calculations, there are some differences in the detail which can influence the results obtained. It seems necessary, for example, to use the generalized gradient approximation (CGA), as opposed to the linear density approximation (LDA) for both the hydride and the H_2 molecule in order to obtain the best accuracy in the calculations. When just looking for trends along a particular transition metal series, however, this may not be too important. Similarly, whilst the calculations over-estimate the cohesive energies of the pure metals, this also may not be too important when the interest lies in the formation energy of the hydride since the error cancels out to a large extent.

The total energy calculations of hydride stability refer to stoichiometric compounds at 0 K and to phases which are defect-free. This should be borne in mind when comparing with the results from experimental measurements where the hydrides often contain large vacancy and dislocation densities. The experimental results for stabilities obtained from plateau pressure measurements are also often influenced by hysteresis.

Although the calculations refer to 0 K, calculations of zero point energies and/or the phonon spectrum gives information on the vibrational contributions to the free energy so that some information on the effect of temperature is obtained. With the same information for the H_2 molecule, information on the temperature variation of the enthalpy of formation can be obtained.

The studies reported to date have either concentrated on particular hydrides formed from rare-earth compounds [21,24,25] or have looked for the factors which

determine stability by looking at trends whilst traversing the Groups across the periodic table [22,23]. Wolverton et al. [26] have examined the Al–H system in detail and have also calculated the stabilities of several other ordered hydrides.

Calculations on disordered phases, of either the host alloy or of the H atom location in ordered compounds is a more difficult exercise. An approximation to such phases can be achieved in the supercell approach in which an ordered superstructure is considered. Here, the size of the unit cell is increased and the occupation within this cell adjusted to the non-stoichiometric composition desired. Mayer et al. [27] have used this method for the calculation of the elastic constants of NbH_x alloys. Calculations of, say, the energetics of the solution of randomly distributed H in a random Pd–Ag alloy would seem to be too much to expect at the moment.

Although their work was concerned principally with the Al–H system, Wolverton et al. [26] performed a series of calculations for the formation energies of 15 binary hydrides which included both transition and non-transition metals as shown in Fig. 5 and Table 4 of their paper. There is very good agreement between calculated and experimental values for the formation energies, especially when the calculated/experimental differences referred to above are taken into account.

Wolverton et al. also found that, in the case of Al–H, the site occupation problem is more complex than previously thought. Both atomic relaxation and anharmonic vibrational effects play an important role in determining the site occupation preference. In unrelaxed calculations, the O-site is preferred, as it is when the higher zero point energy in the T-site is allowed for. However, the energy reduction associated with the larger atomic relaxations around the T-site outweighs these factors making the T-site marginally favored in this system.

Semi-empirical methods, in which the information from total energy calculations and experimental results is mapped onto a pair potential or functional representation, would also seem to have an important role. The Embedded Atom Model (EAM) is the best known method of this type [29]. A set of EAM potentials for used with M–H systems has been assembled by Ruda et al. [30]. With such an energy representation, larger number of atoms can be considered, thus making it possible, for example, to carry out Monte Carlo calculations of the high temperature thermodynamic properties [31] or to consider the energetics associated with extended defects.

A second development which should be mentioned concerns the use of the Calphad method [32] in assessing the thermodynamic properties of M–H systems. In the past, discussions of the thermodynamics of M–H systems have tended to be regarded as a completely separate exercise from a discussion of their phase diagrams. This is apparent from the recent monograph of Manchester and Pitre [33] in which a very thorough assessment for binary M–H systems is carried out. It is clear there, however, that there has been no systematic consideration of the compatibility of the assessed thermodynamic properties of the individual phases with the assessed phase diagram. The Calphad method sets out to rectify this and ensures compatibility between single-phase data and phase diagrams. Gibbs energy minimization packages can be used to optimize the parameters in models used for describing the properties for the individual phases. Since parameters are optimized by considering both the individual phase properties and the phase diagram, compatibility between the two is ensured. Recent assessments by Zeng et al. [34] for the Ni–H system and by Konigsberger et al. [35] for the Ti–H and Zr–H systems, have used this approach for M–H systems.

At the moment there is a problem, in regard to M–H systems, with the models available in the Gibbs energy minimization packages. Site blocking, in which the occupation of an interstitial site is prevented by the prior occupation of a neighboring interstitial site, i.e., there is an effective repulsion between near neighbor H atoms, is an accepted feature in the modeling of some M–H phases. Site blocking gives rise to a large non-ideal entropy of mixing and this can only be estimated either through the use of Monte Carlo simulations [36] or through the use of higher order approximations [37,38]. The models which are available in the Gibbs energy minimization packages, on the other hand, adopt the Bragg–Williams approximation and assume ideal mixing on the interstitial sub-lattice. If the crystallographic value of $\beta = 6$ (β is the number of interstitial sites per metal atom which is 6 for H in T-site occupation in a bcc metal) were to be used with this assumption, then extremely large excess Gibbs energies would be required to fit the experimental results. Rather than do this, it is more straightforward to select a value of β which permits the fitting of experimental results with relatively small values of G^{E}. Whilst this procedure is not as physically satisfying as using a blocking model, it is the best that can be done at present in applying the Calphad method to M–H systems.

Acknowledgement

Professor C.-N. Park is thanked for sharing his valuable insights on the thermodynamic of metal–H systems with TBF over the years.

References

[1] W. Oates, T. Flanagan, Scripta Met. 17 (1983) 983.
[2] C.-N. Park, T.B. Flanagan, Scripta Met. 37 (1997) 1709.
[3] J. Kirkwood, I. Oppenheim, Chemical Thermodynamics, McGraw-Hill, New York, 1961.
[4] F.A. Kuijpers, Philips Res. Rep. Suppl. 2 (1973).
[5] M. Hillert, Jernkont. Ann. 136 (1952) 25.
[6] C.-N. Park, T.B. Flanagan, Ber. Bunsenges. Phys. Chem. 89 (1995) 1300.
[7] P.D. Goddell, J. Less-Common Met. 99 (1984) 1.
[8] P. Dantzer, P. Millet, T.B. Flanagan, Met. Mater. Trans. A 32A (2001) 29.

[9] T.B. Flanagan, W. Luo, J.D. Clewley, J. Less-Common Met. 172 (1991) 42.
[10] B.S. Bowerman, C.A. Wulff, T.B. Flanagan, Z. Physik. Chem. N. F. 116 (1979) 781.
[11] T.B. Flanagan, G. Biehl, J. Less-Common Met. 82 (1981) 383.
[12] W. Luo, J.D. Clewley, T.B. Flanagan, Zeit. Physik. Chem. 179 (1993) 83.
[13] S.N. Klyamkin, V.N. Verbertsky, J. Alloys Compd. 194 (1993) 41.
[14] R. Lasser, K.-H. Klatt, Phys. Rev. B28 (1983) 748.
[15] T. Flanagan, J. Clewley, T. Kuji, C. Park, D. Everett, J. Chem. Soc., Faraday Trans. 82 (1986) 2589.
[16] A. Switendick. In: G. Alefeld, J. Volkl (Eds.), Hydrogen in Metals, I, Springer-Verlag, Berlin, 1978, p. 101.
[17] D.G. Westlake, J. Less-Common Met. 75 (1980) 177.
[18] P. Nordlander, J.K. Norskov, F. Besenbacher, J. Phys. F. Met. Phys. 11 (1986) 1169.
[19] P. Hohenberg, W. Kohn, Phys. Rev. 136 (1964) 864.
[20] W. Kohn, L. Sham, Phys. Rev. 140 (1965) 1133.
[21] K. Tatsumi, I. Tanaka, H. Inui, M. Yamguchi, H. Adachi, Phys. Rev. B 64 (2002) 184105.
[22] K. Miwa, A. Fukumoto, Phys. Rev. B 65 (2002) 155114.
[23] H. Smithson, C. Matienetti, D. Morgan, A. Van der Ve, A. Predith, G. Ceder, Phys. Rev. B 66 (2002) 144107.
[24] L.G. Hector, J.F. Herbst, T.W. Capehart, J. Alloys Compd. 353 (2003) 74.
[25] L.G. Hector, J.F. Herbst, Appl. Phys. Lett. 82 (2003) 1042.
[26] C. Wolverton, V. Ozolins, M. Asta, Phys. Rev. B 69 (2004) 144109.
[27] B. Mayer, M. Methfessel, M. Schott, P. Schmidt, Intermetallics 12 (2004) 333.
[28] G. Kresse, J. Furthmuller, Phys. Rev. B 54 (1996) 11169.
[29] M.S. Daw, M.I. Baskes, Phys. Rev. B 29 (1984) 6443.
[30] M. Ruda, D. Farkas, J. Abriata, Phys. Rev. B 54 (1996) 97.
[31] K.Y. Lee, H.R. Schober, W.A. Oates, Zeit. Physik. Chem. 179 (1993) 1.
[32] N. Saunders, A. Miodownik, CALPHAD. Calculation of Phase Diagrams. A Comprehensive Guide, Elsevier Science, Oxford.
[33] F.D. Manchester, J. Pitre, Phase Diagrams of Binary Hydrogen Alloys, American Society for Metals, Park, Ohio, 2000.
[34] K. Zeng, T. Klassen, W. Oelerich, R. Bormann, J. Alloys Compd. 283 (1999) 151.
[35] E. Koenigsberger, G. Eriksson, W. Oates, J. Alloys Compd. 343 (2002) 243.
[36] W. Oates, J. Lambert, P. Gallagher, Trans. Met. Soc. AIME 245 (1969) 47.
[37] G. Boureau, J. Phys. Chem. 45 (1984) 973.
[38] V. Vaks, N. Zein, V. Kamyshenko, J. Phys. F 18 (1988) 1641.